Clinical Ophthalmology

Dovepress
open access to scientific and medical research

Open Access Full Text Article

ORIGINAL RESEARCH

Assessment of a Novel Semi-Automated Algorithm for the Quantification of the Parafoveal Capillary Network

Zoi Kapsala[1], Aristofanis Pallikaris[1,2], Miltiadis K Tsilimbaris[1,2]

[1]Department of Neurology and Sensory Organs, Medical School, University of Crete, Heraklion, Greece; [2]Vardinoyiannion Eye Institute of Crete, Medical School, University of Crete, Heraklion, Greece

Correspondence: Zoi Kapsala, Department of Neurology and Sensory Organs, Medical School, University of Crete, P.O. Box 2208, Heraklion, 71003, Greece, Email z.kapsala@med.uoc.gr

Clinical Ophthalmology downloaded from https://www.dovepress.com/
For personal use only.

Introduction: We present a novel semi-automated computerized method for the detection and quantification of parafoveal capillary network (PCN) in fluorescein angiography (FA) images.

Material and Methods: An algorithm detecting the superficial parafoveal capillary bed in high-resolution grayscale FA images and creating a one-pixel-wide PCN skeleton was developed using MatLab software. In addition to PCN detection, capillary density and branch point density in two circular areas centered on the center of the foveal avascular zone of 500μm and 750μm radius was calculated by the algorithm. Three consecutive FA images with distinguishable PCN from 56 eyes from 56 subjects were used for analysis. Both manual and semi-automated detection of the PCN and branch points was performed and compared. Three different intensity thresholds were used for the PCN detection to optimize the method defined as mean(I)+0.05*SD(I), mean(I) and mean(I)-0.05*SD(I), where I is the grayscale intensity of each image and SD the standard deviation. Limits of agreement (LoA), intraclass correlation coefficient (ICC) and Pearson's correlation coefficient (r) were calculated.

Results: Using mean(I)-0.05*SD(I) as threshold the average difference in PCN density between semi-automated and manual method was 0.197 (0.316) deg^{-1} at 500μm radius and 0.409 (0.562) deg^{-1} at 750μm radius. The LoA were −0.421 to 0.817 and −0.693 to 1.510 deg^{-1}, respectively. The average difference of branch point density between semi-automated and manual method was zero for both areas; LoA were −0.001 to 0.002 and −0.001 to 0.001 branch points/$degrees^2$, respectively. The other two intensity thresholds provided wider LoA for both metrics. The semi-automated algorithm showed great repeatability (ICC>0.91 in the 500μm radius and ICC>0.84 in the 750μm radius) for both metrics.

Conclusion: This semi-automated algorithm seems to provide readings in agreement with those of manual capillary tracing in FA. Larger prospective studies are needed to confirm the utility of the algorithm in clinical practice.

Keywords: detection, fluorescein angiography, parafoveal capillary network, quantification, semi-automated algorithm

Introduction

The parafoveal capillary network (PCN) constitutes a microvascular network surrounding the foveal avascular zone (FAZ) of the macula. It represents an important, complex, retinal microstructure that covers the metabolic needs and controls immune reactions of the inner retinal layers. The PCN is often compromised in several retinal diseases even in the early stages.[1] The microangiopathy of PCN leads to the development of significant consequences including ischemia of the macula, which can be threatening for the visual acuity.[2] Therefore, the imaging and assessment of this structure is of great importance for monitoring the retinal function in various retinal vascular diseases.

Many researchers have studied PCN and have proposed metrics for quantifying its morphology and any possible alterations. The usefulness of assessing and quantifying macular ischemia is well documented in retinal vasculopathies such as diabetic retinopathy and retinal vein occlusions.[3–8] Specifically, metrics reflecting capillary network integrity have been recently studied in normal and pathologic retinas and include regularity of shape and size of FAZ, density of

Received: 12 February 2023
Accepted: 1 May 2023
Published: 8 June 2023

© 2023 Kapsala et al. This work is published and licensed by Dove Medical Press Limited. The full terms of this license are available at https://www.dovepress.com/terms.php and incorporate the Creative Commons Attribution – Non Commercial (unported, v3.0) License (http://creativecommons.org/licenses/by-nc/3.0/). By accessing the work you hereby accept the Terms. Non-commercial uses of the work are permitted without any further permission from Dove Medical Press Limited, provided the work is properly attributed. For permission for commercial use of this work, please see paragraphs 4.2 and 5 of our Terms (https://www.dovepress.com/terms.php).

capillary network, density of capillary branch points and perifoveal intercapillary area.[4,6,9–13] It has been postulated that many of these metrics have diagnostic and prognostic value in diseases affecting retinal microcirculation. Hence, research has been directed toward the improvement and automation of algorithms that analyze images of the capillary bed and calculate parameters that quantify its morphology. These new tools may play an essential role in routine clinical practice in the near future.

In our previous work, we developed a novel algorithm to manually assess the morphology of PCN in fluorescein angiography (FA) images of young patients with diabetes mellitus type I. This was a preliminary study in which we calculated the PCN density, branch point density and FAZ area. The manual procedure showed high repeatability, while the capillary metrics were confirmed to differentiate between normal and pathologic.[9]

In this article, we present and evaluate our effort to accelerate the detection of the PCN, automating the manual algorithm presented previously. Therefore, we describe a novel semi-automated algorithm that constitutes the evolution of this initial manual method, and traces the PCN in FA images and calculates the PCN density and the density of branch points in two circular areas centered on the center of the FAZ of 500μm and 750μm radius. The performance of our algorithm was assessed by estimating the repeatability, correlation and agreement with a manual detection process. Hence, this constitutes a study of the feasibility of a novel semi-automated algorithm to detect and quantify PCN in FA images. In the recent past, many efforts have been recorded regarding the quantification of PCN using non-invasive imaging techniques, for instance optical coherence tomography-angiography (OCT-A), which tend to be in wide use, as they are not associated with the adverse reactions of an intravenous dye administered in an FA and provide clear depiction of both superficial and deep capillary networks. However, FA is considered to image clearly only the superficial capillary network. Nevertheless, FA is still considered the gold standard imaging method in retinal vascular diseases and an imaging adjunct to non-invasive techniques in several retinal vascular cases. Therefore, since progress on the validation and optimization of algorithms analyzing FA images is incomplete, this study could add to the current knowledge regarding parafoveal capillary segmentation in FA images.

Materials and Methods

Participants

FA images meeting specific criteria were selected retrospectively from the digital database of the University Hospital of Heraklion. FA images from eyes with either normal or pathologic capillary morphology were eligible for our analysis. Eyes with spherical equivalent higher than ±3.00 D, undergone ocular surgery, presented media opacities as well as extensive macular disease obscuring PCN imaging and capillary metrics detection and quantification, including any macular vascular disease extensively distorting the FAZ, were excluded from the study. We preferred images of the macula captured during the arteriovenous phase of the FA examination. As a study eye for each subject, we selected the one with the clearest depiction of PCN. The 3 FA images with the most distinguishable PCN depiction (out of a range of 3 to 7 images per person) were identified for the study eye of each subject and exported in JPEG format for further analysis. The study was performed in adherence to the tenets of the Declaration of Helsinki. Written informed consent was obtained on a subsequent visit after FA from all participants (or subject's parents if younger than 18 years old) after discussing the purpose and the nature of the study. The protocol was also approved by the Institutional Review Board at the University General Hospital of Heraklion.

Ophthalmic examination data including best corrected visual acuity (BCVA), Goldmann applanation tonometry, biomicroscopy of anterior segment, dilated fundus examination and FA as well as demographic data and indication to undergo FA were obtained from subjects' medical records. Both patients' data and exported FA images were analyzed anonymously.

Fluorescein Angiography

Fluorescein angiography (a 5-sec bolus injection of 5mL 10% dye) was performed after dilating the pupil with a combination of tropicamide 0.5% and phenylephrine 5% eye drops. A single, well-trained ophthalmic photographer acquired all FA images analyzed in this study and followed a standardized imaging protocol for all subjects. FA images

of 50° field were obtained using a TRC-50DX Type IA Topcon fundus camera (Topcon, Tokyo, Japan). The optical system used had a resolution of 3.2 Megapixels. FA images of the macula were taken once every second for about 20 sec and then, less often. Imaging of the fellow eye occurred between 30 and 50 sec. Mid-phase images (1–5 min) of both eyes were also obtained every 30 sec, while a late FA image of each eye was captured at 5 and 10 min.

Image Analysis

The algorithm was written in commercially available software (MATLAB; The MathWorks Inc., Natick, MA). Initially, the algorithm accepts the original FA image of resolution 1900×1472 pixels in .jpg format (Figure 1A). A rough estimate of the center of the FAZ is performed automatically using a spatial correlation of the image with a Gaussian structure and a cropped subimage of 287×287 pixels surrounding the FAZ is produced for further analysis (Figure 1B). Subsequently,

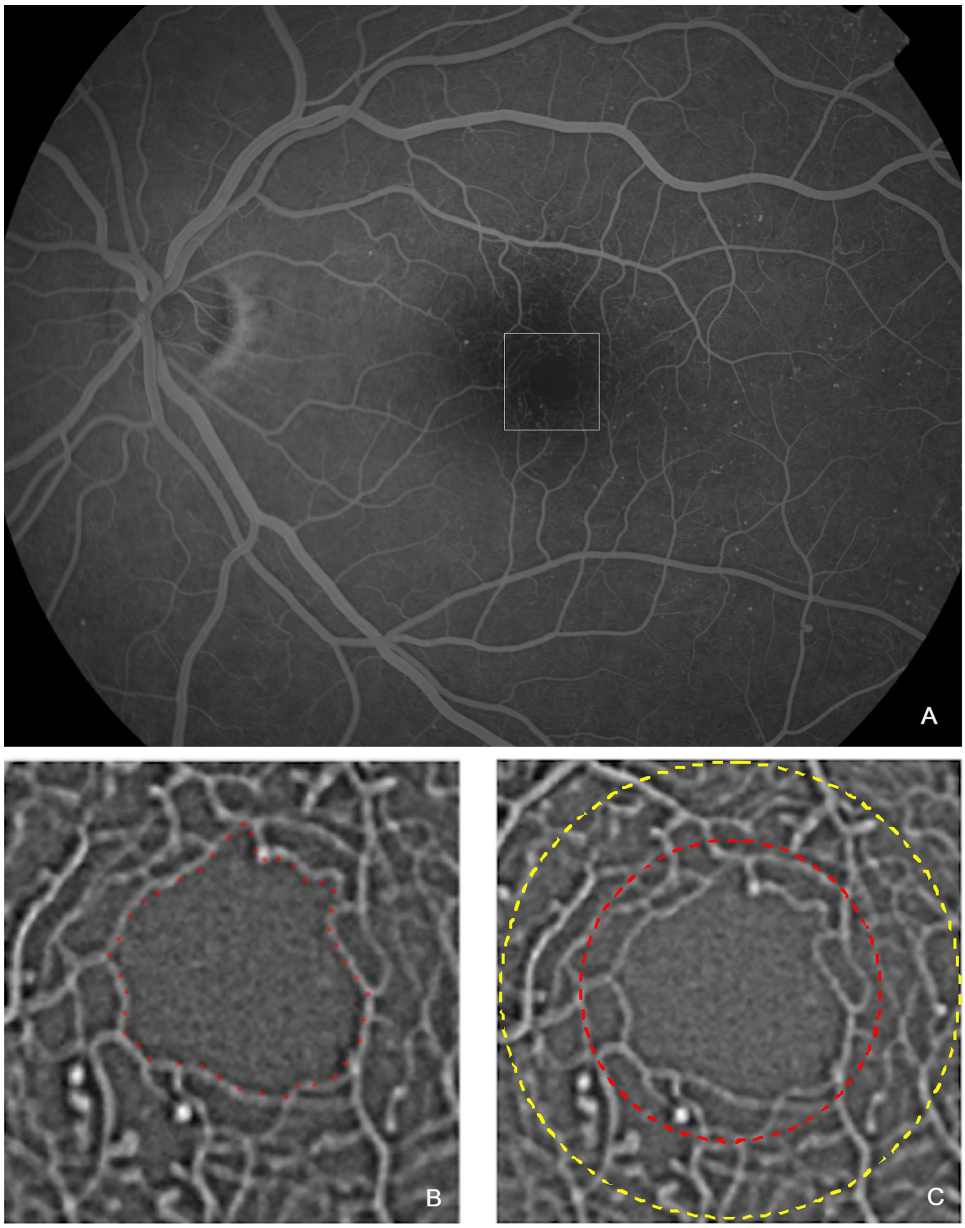

Figure 1 Original FA image (**A**) of 1900×1472 pixels from the left eye of a 34 year-old female subject with non-proliferative diabetic retinopathy and cropped subimage (**B**) of 287×287 pixels in which the border of the FAZ was delineated manually (red dots in (**B**)) to initiate the detection and quantification process. The white dashed square indicates image 1B. The two circular ROIs of 500μm and 750μm radius are depicted in (**C**) (red and yellow dashed circle, respectively).

the user traces the outline of the FAZ in a manual manner in this subimage and the final cropped image (208x208 pixels) centered at the centroid of the FAZ is produced. This image is initially filtered by a Gaussian filter to suppress noise and then, filtered with a Frangi filter that enhances tubular structures such as vessels.[14,15] Finally, a binary image delineating the PCN is created by applying an intensity threshold to the final filtered image and a one-pixel-wide skeletonized version of the PCN is produced. For the current study, three different thresholds were applied to optimize the method, so that it provides values close to the manual procedure. The three thresholds for each image were defined as follows: mean(I)+0.05*SD(I), mean(I), mean(I)-0.05*SD(I), where I is the grayscale intensity of the image analyzed and SD the standard deviation. These thresholds were selected after applying various threshold values of intensity on FA images from 10 subjects. After this short pilot study, we selected the threshold value (adding and subtracting 0.05*standard deviation) that provided results of PCN metrics very close to those after manual detection.

The manual procedure has been previously described.[9] In the work presented here, the manual algorithm was applied to the extracted images before semi-automated algorithm by the same unique tracer for all images. The tracer performing the manual detection was also blind to the data during the procedure.

Calculation of PCN Morphology Metrics

Assessment of PCN integrity was performed by calculating two quantitative measures: the PCN density and the density of branch points.

PCN Density

This parameter has been defined previously as tcL/A, where tcL=total capillary length in degrees in region of interest (ROI)[9] and A=ROI-FAZ in degrees^2. PCN density does not quantify the number of capillaries per unit area. Instead, it represents the length of PCN in a ROI per unit area.

Branch Point Density

Density of branch points was defined as the number of capillary branch points in a specified area divided by the same surface in degrees^2 excluding the surface of the FAZ.

The capillary measures were quantified in two central circular ROIs considered from the centroid of the FAZ after excluding the FAZ area from our calculations, a ROI of 500 μm radius and a larger one of 750μm radius (Figure 1C). Both metrics were estimated for all three different image intensity grayscale thresholds mentioned above to determine the one that provides results closest to the manual process.

Statistics

The intraclass correlation coefficient (ICC)[16] for the two capillary network parameters was calculated as an index of repeatability of the algorithm after analyzing three consecutive FA frames from a single FA of the same eye for each one of the subjects with the semi-automated and the manual image processing algorithm. Besides calculating the repeatability of the manual procedure on three consecutive FA frames, we estimated the repeatability by manually detecting the PCN and branch point density on the same FA image three times. The ICC calculation for the metrics mentioned above was independent from the repeatability of the manual FAZ detection process, as the ICC for the last was 99.9%.[9] Thereafter, within subject standard deviation was also calculated for each metric and method, as an index of measurement error.[17] To assess the extent of agreement between the semi-automated and the manual methods limits of agreement (LoA), allowing for repeated measurements per eye,[18] were calculated for PCN and branch point density. Narrower limits indicate closer agreement. Bland-Altman plots were constructed.[19] Mean differences were calculated (using the average of the three measurements). Pearson's correlation coefficient (r) was calculated to assess the linear correlation between PCN and branch point density resulting from the semi-automated process and those resulting after manual capillary and branch point tracing using the mean value of the three repeated measurements. Sample size was determined based on literature regarding statistical analysis of repeated measurements, which suggests that a minimum sample of 50 is acceptable.[20] Moreover, power of correlations was estimated post hoc using statistical package GPower 3.1.9.7. Statistical analysis described above was performed for both 500 and 750μm radius areas and for all three grayscale image intensity

Table 1 Indications for Performing FA in the Study Group

Indications for Performing FA	Number of Eyes
Diabetes mellitus	36
Retinal vein occlusion	8
Central serous choroidopathy	5
Choroidal nevus	4
Posterior uveitis	2
Age-related macular degeneration	1
Total	56

thresholds. Data are presented as means ± standard deviations (range) and all analyses were performed using IBM SPSS Statistics software version 23 (SPSS Inc., Chicago, IL). For all tests, $p<0.05$ was considered statistically significant.

Results

FA images from 56 eyes from 56 subjects meeting the specified criteria were included in our analysis. The study group consisted of 32 males and 24 females aged 47±15 years (range: 12–73 years). BCVA was 0.07±0.12 logMAR (range: 0–0.70 logMAR). Thirty-six of the 56 subjects (64%) had a history of diabetes mellitus (DM) for 16±7 years (range: 4–32 years). Fifteen of the 36 diabetic subjects presented DM type 1 and 21 subjects had DM type 2. Findings of DR (ranging from mild to severe non-proliferative DR) have been detected in 22 out of the 36 eyes (61%) of DM subjects. Twenty subjects (36%) underwent FA investigation for a retinal pathology other than diabetic retinopathy (DR) that did not interfere with the clarity of the PCN, and thus with the detection and quantification of capillary metrics by the algorithm. Indications for undergoing FA in our study are summarized in Table 1.

An example of application of the algorithm on an original FA image (Figure 1) to detect and quantify the PCN and branch points for the three selected grayscale image intensity thresholds is depicted in Figures 2 and 3, respectively.

ICC values and 95% confidence intervals of PCN and branch point density in 500 and 750 μm radius areas resulting after processing FA images with the semi-automated and manual algorithms are included in Table 2. Applying the semi-automated algorithm, the area of 500 μm radius yielded ICC values higher than 0.909 for both metrics and among all applied grayscale thresholds, whereas the respective results for the larger area of 750 μm radius were ranging between

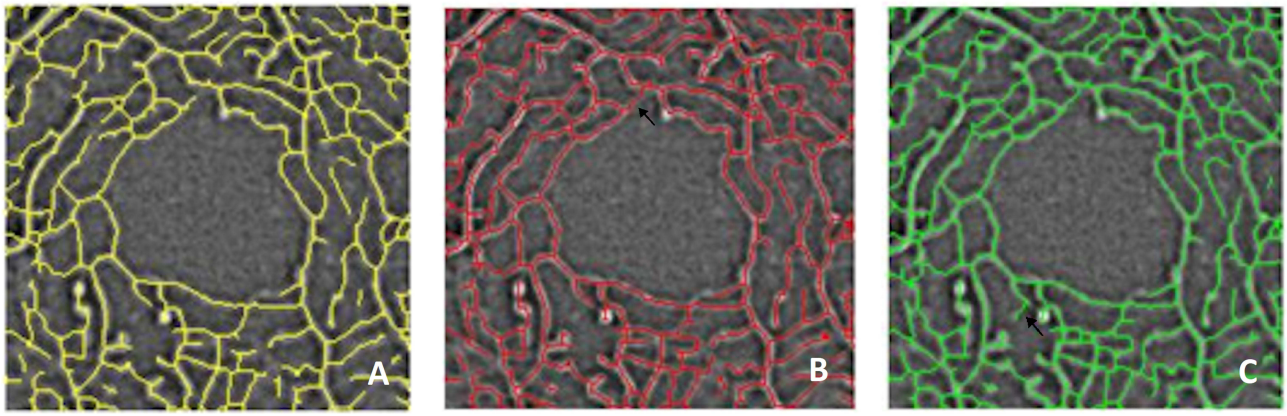

Figure 2 Figures illustrate the automatically detected PCN as a one-pixel-wide skeleton in a subimage of 208×208 pixels. This procedure was performed for three different image intensity grayscale thresholds of progressively lowering value from left to right (**A-C**). Arrows in (**B** and **C**) are pointing examples of PCN parts detected for the specific image grayscale threshold used, but were missed in (**A** and **B**), respectively.

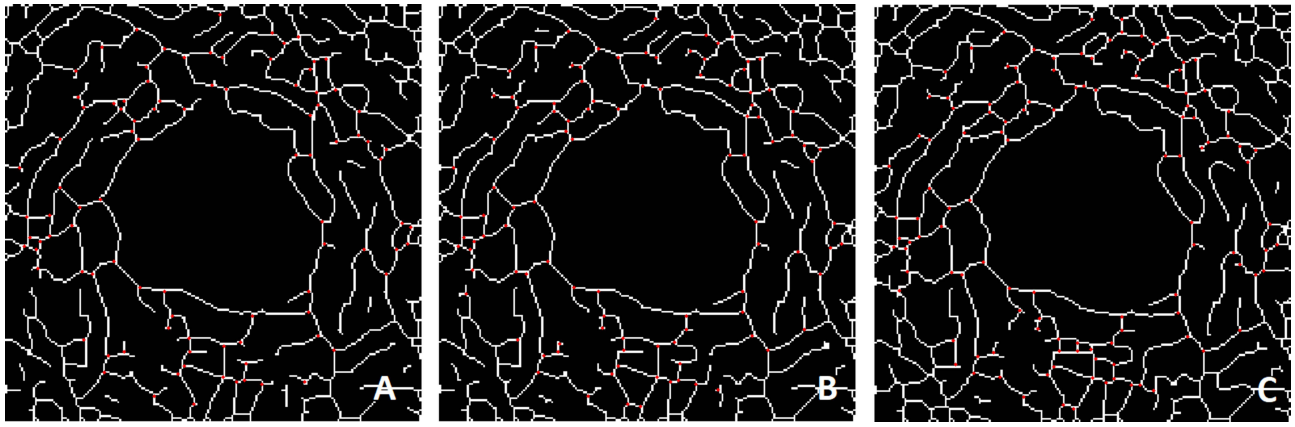

Figure 3 Detection of branching points (red dots) on the automatically traced and skeletonized capillary network (white lines). Network traced in (Figure 3**A-C**) coincides with that illustrated in (Figure 2**A-C**), respectively, and results from progressively lowering image intensity grayscale thresholds from left to right.

0.837 and 0.893. Repeatability of the manual procedure was very high after applying it on three consecutive FA images with clear depiction of PCN as well as after application on the same FA image 3 times.

Within subject standard deviations for the PCN and branch point density are mentioned in detail in Table 3. Noteworthy, this index regarding the branch point density in both zones was lowest and closest to the manual results for threshold 3. Regarding the PCN density in 500μm zone, within subject standard deviation for thresholds 1 and 3 was found to be closer to the manual one, whereas in 750μm zone, the index yields gradually higher values from threshold 1 to threshold 3.

Table 4 presents the LoA for PCN and branch point density in the studied areas around the FAZ and for all image grayscale thresholds applied. Mean difference of PCN density calculated by the semi-automated algorithm and the

Table 2 ICC After Assessing the Repeatability of the Semi-Automated and the Manual Method for the Calculation of PCN Density and Branch Point Density. 95% Confidence Intervals of ICC are Presented in Parentheses. Table Includes Results for All Three Grayscale Thresholds Applied and for Both ROIs of 500 and 750 μm Radius. All Results Below Were Statistically Significant, as p-value Was <0.001 for Each Separate Calculation of ICC

	PCN Density		Branch Point Density	
	500μm	750μm	500μm	750μm
Threshold 1	0.964 (0.937–0.979)	0.837 (0.723–0.905)	0.914 (0.870–0.946)	0.884 (0.872–0.891)
Threshold 2	0.935 (0.894–0.961)	0.843 (0.746–0.905)	0.909 (0.863–0.942)	0.884 (0.868–0.892)
Threshold 3	0.962 (0.926–0.980)	0.872 (0.801–0.920)	0.921 (0.881–0.950)	0.893 (0.883–0.896)
Manual (3 consecutive FA images)	0.983 (0.973–0.989)	0.944 (0.914–0.965)	0.935 (0.902–0.959)	0.891 (0.880–0.895)
Manual (same FA image)	0.994 (0.982–0.998)	0.944 (0.847–0.984)	0.946 (0.852–0.985)	0.837 (0.615–0.952)

Table 3 Within-Subject Standard Deviation for Density of PCN (Degrees^{-1}) and Branch Point (Branch Points/degrees^{2}) in Both Areas and for All Grayscale Thresholds Applied

	PCN Density		Branch Point Density	
	500μm	750μm	500μm	750μm
Threshold 1	0.195	0.228	0.008	0.004
Threshold 2	0.291	0.251	0.007	0.004
Threshold 3	0.199	0.269	0.004	0.002
Manual	0.146	0.188	0.002	0.001

Table 4 Average Difference of Measurements Between Semi-Automated and Manual Process, Standard Deviation of Difference in Parentheses and Limits of Agreement (at the Second Line of Each Cell) of PCN Density (in Degrees^{-1}) and Branch Point Density (in Branch Points/degrees^2) for Each One of the Three Image Intensity Grayscale Thresholds in the 500 and 750 μm ROIs

	PCN Density		Branch Point Density	
	500μm	750μm	500μm	750μm
Threshold 1	−0.143 (0.459) −1.044 to 0.759	−0.150 (0.619) −1.366 to 1.065	−0.002 (0.003) −0.006 to 0.002	−0.002 (0.002) −0.006 to 0.001
Threshold 2	0.097 (0.464) −0.843 to 0.977	0.127 (0.589) −1.027 to 1.281	−0.001 (0.002) −0.004 to 0.002	−0.001 (0.002) −0.005 to 0.002
Threshold 3	0.197 (0.316) −0.421 to 0.817	0.409 (0.562) −0.693 to 1.510	0.000 (0.001) −0.001 to 0.002	0.000 (0.001) −0.001 to 0.001

manual method in the 500μm area were −0.143, 0.097 and 0.197 degrees^{-1} for the three respective grayscale thresholds. The respective results for the larger area of 750 μm radius were −0.150, 0.127 and 0.409 degrees^{-1}. Additionally, mean difference of branch point density in the 500μm area was −0.002, −0.001 and 0 branch points/degrees^2 for the three respective grayscale thresholds, and −0.002, −0.001 and 0 branch points/degrees^2 in the 750μm radius zone. Mean differences for both metrics and for all grayscale thresholds presented approximately normal distribution. Good agreement was noted for all grayscale thresholds, but threshold 3 provided the narrowest LoA regarding both capillary metrics. Specifically, LoA provided by applying threshold 3 were calculated to range from −0.421 to 0.817 and −0.693 to 1.510 degrees^{-1}for the PCN density in the 500μm and 750μm radius areas, respectively. LoA for the same threshold were found ranging from −0.001 to 0.002 and −0.001 to 0.001 branch points/degrees^2 for the branch point density in the 500μm and 750μm radius areas, respectively. Figures 4 and 5 represent Bland-Altman plots for PCN density after applying the semi-automated and manual algorithms in 500μm and 750 μm radius zones, respectively. Figures 6 and 7 constitute Bland-Altman plots regarding branch point density in the above mentioned areas, respectively. All these diagrams concern threshold 3, which provided the narrowest LoA.

Furthermore, results of linear correlation between semi-automated method and manual capillary detection regarding both PCN and branch point density are presented in Table 5. Pearson's correlation coefficient ranged from 0.919 to 0.999 for branch point density in both analyzed areas. Regarding PCN density, the same coefficient was comparably high in the 500μm radius area ranging between 0.909 and 0.959 and fair in the 750μm radius area ranging from 0.628 to 0.697.

Power for comparisons between semi-automated and manual methods was calculated through GPower to be over 99% for all comparisons (a-probability error=0.05).

Discussion

In this article, we describe a novel semi-automated method that detects the capillary network surrounding FAZ by processing FA images. Additionally, the proposed algorithm calculates the density of PCN and branch points in two central areas of the macula of 500μm and 750μm radius as two indices of capillary network morphology that reflect capillary dropout. The performance of our algorithm has been evaluated by estimating the agreement with the manual method as well as the repeatability and the correlation between semi-automated and manual algorithm.

The algorithm provided highly repeatable measurements for both metrics and for all grayscale image intensity thresholds in the 500μm ROI, which were close to the results of manual delineation procedure. Regarding the larger area of 750μm, ICC was slightly lower than 500μm zone, but still high for both metrics and for all applied grayscale thresholds. Noteworthy, lower threshold values yielded slightly higher ICC results for both metrics. Measurements of PCN density in the area of 500μm radius as well as calculations of branch point density in both areas after processing with the semi-automated method correlated highly with the manual tracing method. However, the semi-automatic method

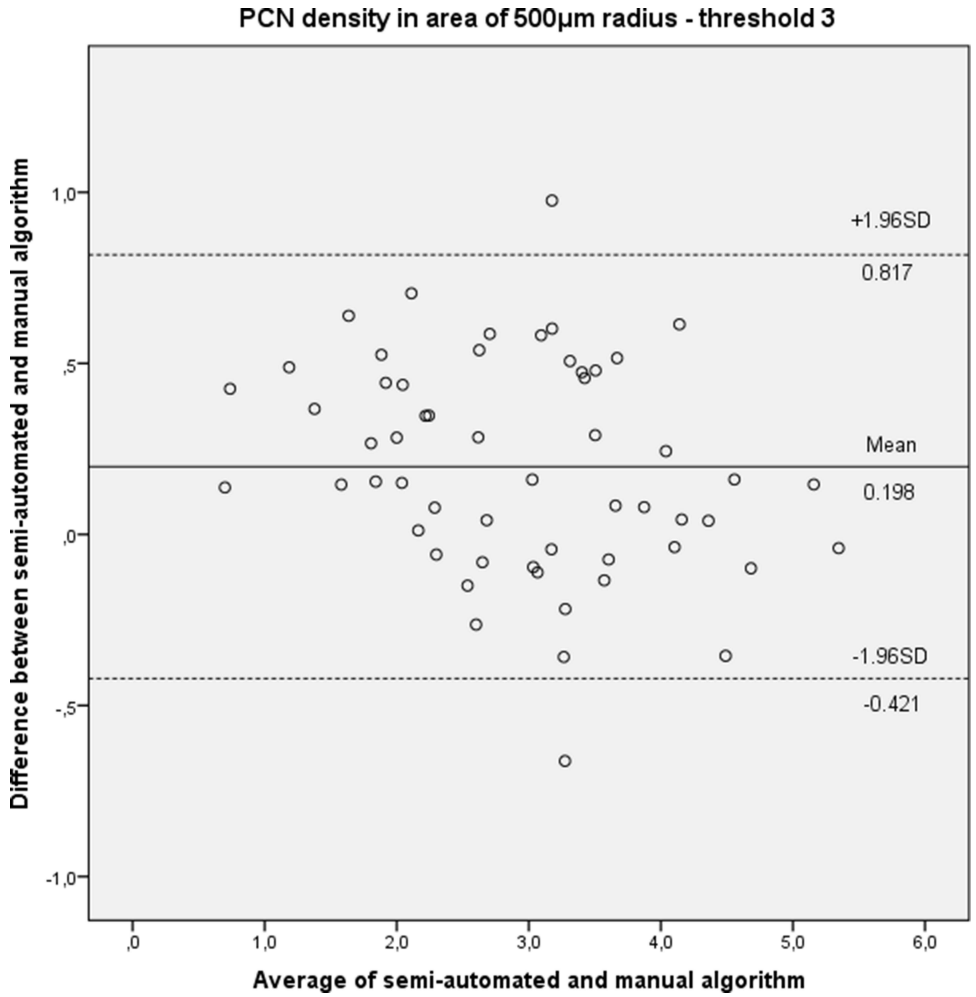

Figure 4 Bland-Altman plot presenting mean difference (solid line) and limits of agreement (upper and lower dashed lines) of PCN density (in degrees^{-1}) between semi-automated and manual algorithm applying threshold 3 in the 500μm radius area.

provided measurements of PCN density in the area of 750μm radius that correlated fairly with the results of the manual procedure. All three grayscale image intensity thresholds yielded similar results and, interestingly, it was found that better correlation with the manual method was achieved for lower threshold values. The same trend was detected after calculating the LoA for all studied metrics and ROIs. The lower the image threshold is, the narrower the LoA are. This means that the highest agreement between semi-automatic and manual methods was achieved for the lowest image grayscale threshold applied, indicating that the application of lower intensity threshold values enabled the detection of a greater part of the capillary plexus around the FAZ as well as the branch points in both ROIs.

The proposed methodology for the quantification of PCN and branch points provided encouraging results and offers several advantages compared to manual detection methods. Among them, the most important is the ability to quickly detect and quantify the network surrounding the FAZ, avoiding the time-consuming manual detection of retinal capillaries. Considering this opportunity and the fact that the studied parameters have been previously confirmed to be sensitive enough to detect capillary abnormalities,[9] this method could have applications in clinical medicine for the diagnosis and monitoring of the progression of many retinal vascular diseases, the establishment of potential disease biomarkers or the improvement of understanding the pathophysiologic mechanisms underlying the capillary dropout process. The fair agreement of semi-automated algorithm with the manual method regarding the PCN density calculations in the ROI of 750μm radius could possibly be explained by the higher complexity of the capillary plexus far from the FAZ compared to the network close to it.

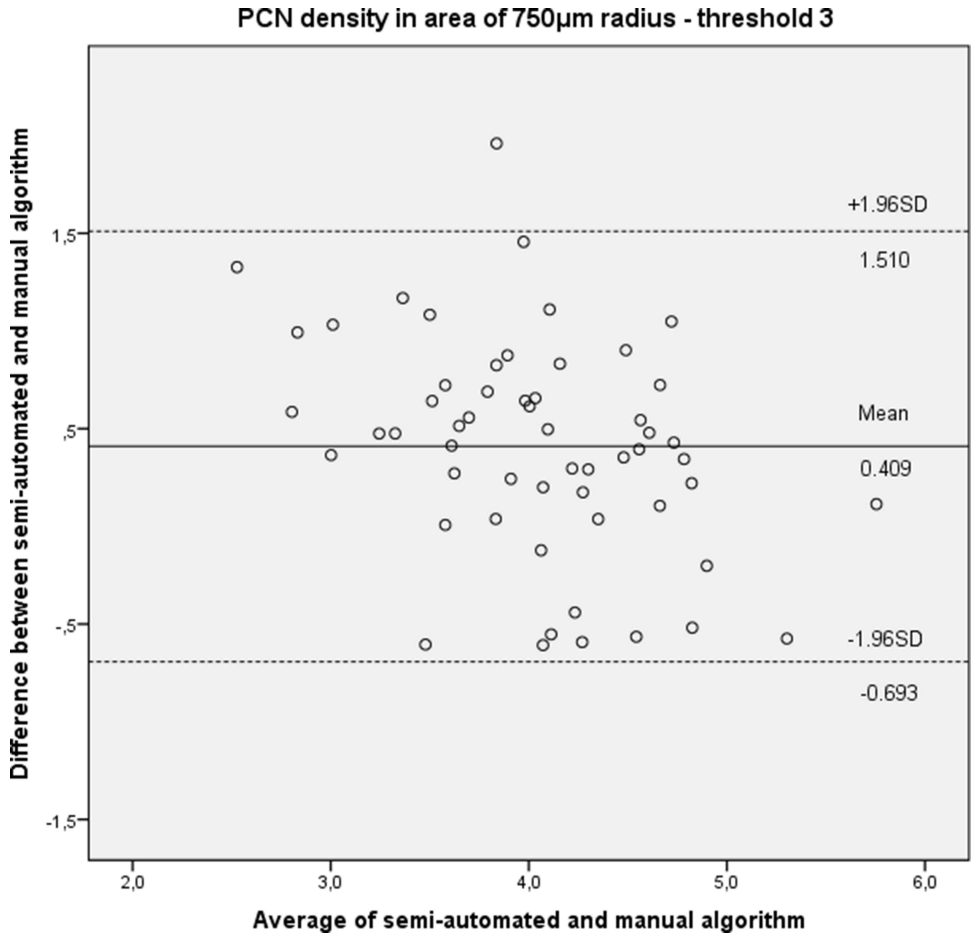

Figure 5 Bland-Altman plot presenting mean difference (solid line) and limits of agreement (upper and lower dashed lines) of PCN density (in degrees^{-1}) between semi-automated and manual algorithm applying threshold 3 in the 750μm radius area.

An important limitation of our study was the need for an intravenous contrast agent, ie fluorescein, to visualize the PCN. The invasive nature of the FA implies that in rare instances it could be accompanied by several adverse events. Novel noninvasive technologies permit the imaging of the retinal microvasculature avoiding complications related to the intravenously administered dye. These new imaging modalities include optical coherence tomography angiography (OCT-A), ultrahigh-resolution optical coherence tomography with adaptive optics (UHR-AO-OCT),[1] dual-conjugate adaptive optics[11] and retinal function imager (RFI).[21] Among them, OCT-A has been introduced in daily clinical practice and has the potential to be an alternative to FA for several retinal vasculopathies. OCT-A is based on motion contrast instead of injecting an intravenous contrast dye to generate angiograms of the fundus comparable qualitatively and quantitatively to the FA, the current gold standard.[22–24] OCT-A provides a clear depiction of both superficial and deep capillary networks, whereas FA images adequately only the superficial capillary network. Studies on normal subjects or diabetic patients using OCT-A support that it is characterized by satisfactory repeatability and sensitivity and could detect retinal vascular diseases at an early stage.[24–28] Recently, efforts to register images of a specified retinal area resulting from FA and OCT-A have been recorded. It was concluded that these imaging modalities complement each other successfully regarding imaging and interpretation of vascular diseases, as success rate was 98.8% and best mean execution time was less than 5 sec per image.[29] The ease of new non-invasive imaging techniques including OCT-A has contributed to great progress and improvement in algorithms that quantify the PCN using these methods. However, only minimal progression has been recorded regarding PCN segmentation using FA, which still could not be replaced completely by new technologies despite evolution in retinal vascular imaging.[30–32] The majority of these studies concern diabetic retinopathy. Among them, Elrashidy et al concluded that FA and OCT-A are comparable regarding

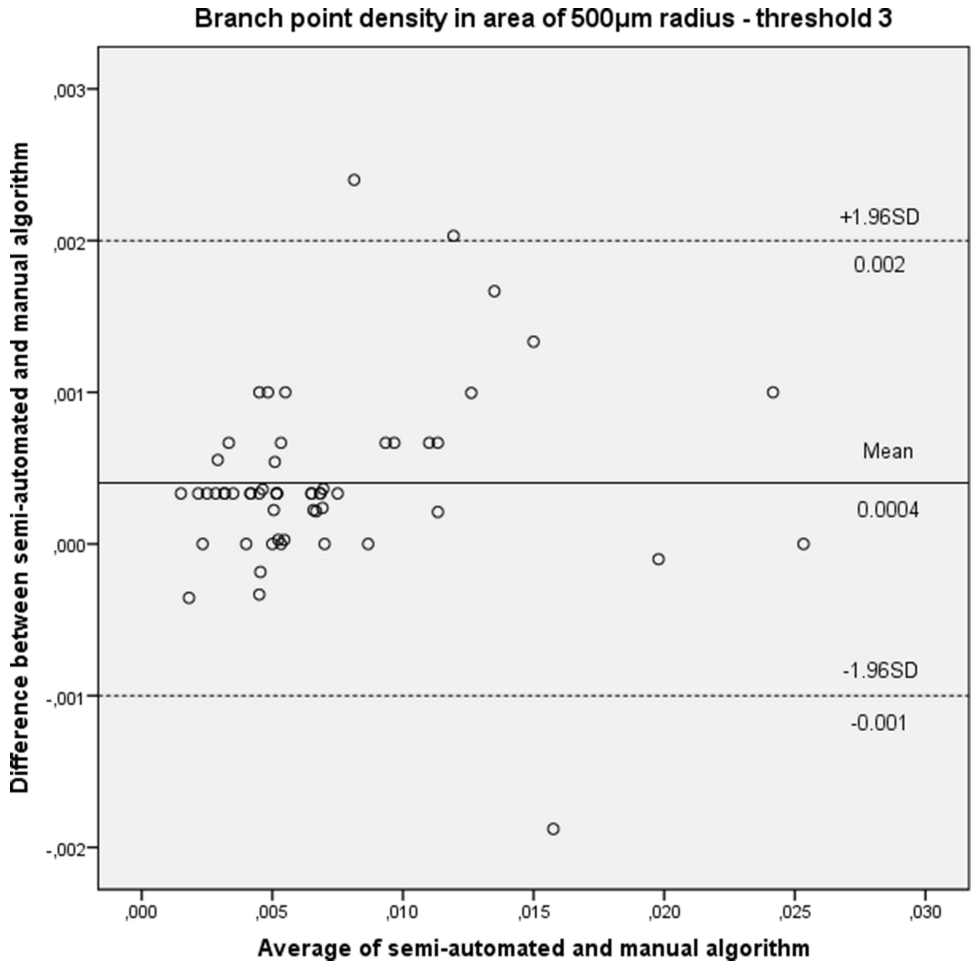

Figure 6 Bland-Altman plot showing mean difference (solid line) and limits of agreement (upper and lower dashed lines) of branch point density (in branch point/degrees^2) between semi-automated and manual algorithm applying threshold 3 in the 500µm radius area.

microaneurysm and capillary non-perfusion detection.[33] Moreover, Bawany et al noted a correlation between automated vessel density detection and vision in proliferative diabetic retinopathy patients.[34] Abbasnejad et al studied diabetic retinopathy patients and recorded reduced retinal blood flow and increased permeability as the earliest signs of diabetic retinopathy using a computer-aided algorithm that analyzes FA images.[35] Additionally, deep learning segmentation has been used for the quantification and staging of capillary non-perfusion[36] and for evaluation of FA images in DR patients.[37,38] Apart from segmentation of FA images for capillary network morphology, advances have also been performed in automated detection of vascular leakage.[39]

Several researchers have published works related to the development and improvement of algorithms for the quantitative assessment of the FAZ or the capillary bed surrounding FAZ analysing images obtained by invasive and non-invasive imaging modalities. The main limitation of these works relates to the lack of algorithm validation. To our knowledge, validation has rarely been presented in the past and concerns mostly PCN metrics assessed using OCT-A. Among them, Boe et al developed and described a deep learning algorithm that distinguishes nonperfusion areas from areas of low signal on OCT-A images. They concluded that the method presented high sensitivity and specificity, which were independent from DR stage and image quality.[40] Iafe et al quantified capillary density and FAZ area in OCT-A scans from normal subjects and validated the reproducibility of these metrics.[41] Additionally, intervisit repeatability of the same metrics was validated later by Garrity et al.[42] Coscas et al validated both interobserver reproducibility and intraobserver repeatability, revealing high values in both superficial and deep capillary plexus in OCT-A scans from healthy subjects.[43] Yu et al compared OCT-A scans with high-resolution confocal microscope images of retinal capillary

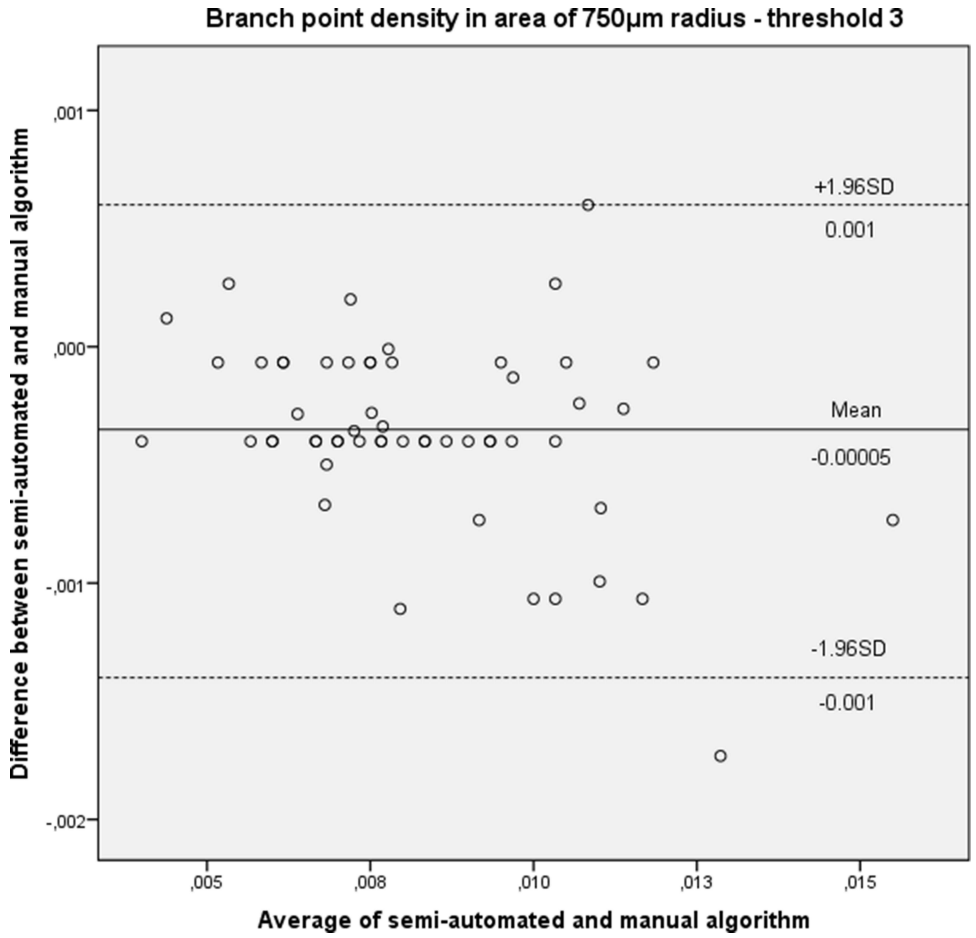

Figure 7 Bland-Altman plot illustrating mean difference (solid line) and limits of agreement (upper and lower dashed lines) of branch point density (in branch point/degrees^2) between semi-automated and manual algorithm applying threshold 3 in the 750µm radius area.

plexus from porcine eyes. They validated in this way metrics, such as vessel length, vessel diameter and branch points. Moreover, there is no recorded attempt so far to quantify the amount or density of parafoveal branching points as a macular ischemia index in images from human eyes. There is only one report from Yu et al, who analyzed images from porcine eyes, as mentioned above and detected that OCT-A tends to underrepresent branch points rather than histology.[44] Zheng et al created a semi-automated segmentation method to quantify the FAZ in FA images from patients with different grades of diabetic retinopathy. This program required manual initiation and yielded reproducible and highly

Table 5 Results of Linear Correlation (Pearson's Correlation Coefficient) Between the Semi-Automated and the Manual Method Concerning Calculation of PCN Density and Branch Point Density for the Three Grayscale Thresholds in the 500 and 750 µm ROIs. p-value Was <0.001 for All Comparisons Below

	PCN Density		Branch Point Density	
	500µm	750µm	500µm	750µm
Threshold 1	0.909	0.628	0.998	0.919
Threshold 2	0.912	0.665	0.999	0.971
Threshold 3	0.959	0.697	0.999	0.999

correlated results with those of manual FAZ detection.[45] Furthermore, Hwang et al assessed the repeatability of the automated algorithm analyzing two scans obtained during the same visit and distinguished eyes with diabetic retinopathy from healthy eyes by analyzing OCT angiograms and calculating FAZ area, total avascular area, perifoveal and parafoveal capillary density in the central 5mm-diameter surface. In another study, Lopes de Faria et al concluded that RFI could quantify reproducibly the perifoveal capillary network after analyzing images from healthy subjects using the Otsu's method. ICC was calculated between 0.879 and 0.968 ($p<0.001$). The presented method required the manual delineation of the FAZ to initiate capillary detection.[21]

Considering the above progression in retinal vascular imaging, our algorithm could be applied not only on FA images but also on images acquired using these new noninvasive imaging techniques after certain adjustments, provided that images of adequate quality are exported for processing. Image quality constitutes a potentially significant drawback for the majority of imaging technologies including FA, AO-SLO and OCT-A, since intraocular scattering and absorption have a strong impact on the quality of images.[22] Situations affecting image quality may include small pupil, media opacities and poor subject cooperation, which may be common in older subjects. Hence, it would be of great interest and importance to apply our algorithm on images acquired through these new non-invasive imaging modalities eg OCT-A and to compare the measurements provided with those resulting from application on FA images.

Our decision on using a global thresholding approach based on the mean intensity value of the image and its standard deviation may be considered as oversimplified and a limitation to our study. Despite this fact, it is important to note that this approach was based on adequate information that originated from our initial pilot examination on 10 subjects, and images were properly selected and denoised to have high contrast quality. The steps prior to applying thresholding to the images permit such an oversimplified approach as illustrated by the end results. To fine-tune the analysis a more complicated thresholding approach should be considered in future similar research work, now that the proof of concept has been illustrated by our results.

Another point of our analysis that should be discussed is the sample size, which consisted of 56 subjects. Although the recommended number for method agreement studies is often at least 100,[46] a recent recommendation when 3 repeats are available is 50.[20] In addition, the study presented was retrospective. Therefore, it should be considered a first step in the process of assessing the feasibility of an automated algorithm to quantify the parafoveal capillary network. Additionally, since only FA frames with clear depiction of the capillary network were further analyzed, the wide age range of the sample as well as the variety of posterior segment diseases had no effect on image quality and clarity. Thus, age and disease did not constitute confounders for the assessment of the algorithm. Moreover, the need for manual tracing of the terminal capillary vessels defining FAZ to initiate the PCN and branch points detection process may still introduce some degree of subjectivity. The automation of FAZ mapping could address this limitation, and we plan to introduce it in our future work as a modification of the current algorithm. Furthermore, there was only one single manual tracer of the PCN and one single photographer acquiring the FA images. Thus, possible inter-rater effects could not be assessed, but they will be in a definitive study. Finally, since axial length measurements were not available for every subject included in the study, all calculations have been performed and presented in degree units instead of μm, which is nevertheless an objective and robust unit resulting after conversion from pixel dimensions.

In conclusion, the work presented in this article constitutes the evolution of our attempt to quantify the parafoveal capillary network. The evaluated algorithm has the potential to automatically detect and calculate quickly and precisely capillary parameters quantifying the morphology of the parafoveal capillary plexus. Thus, it becomes evident that the application of such an algorithm in further research and ideally in routine clinical practice could accelerate clinical assessments, staging and management of patients.

Funding

There was no funding for this study.

Disclosure

The authors report no conflicts of interest in this work.

References

1. Wang Q, Kocaoglu OP, Cense B, et al. Imaging retinal capillaries using ultrahigh-resolution optical coherence tomography and adaptive optics. *Invest Ophthalmol Vis Sci*. 2011;52(9):6292–6299. doi:10.1167/iovs.10-6424
2. Takahashi K, Kishi S, Muraoka K, Shimizu K. Reperfusion of occluded capillary beds in diabetic retinopathy. *Am J Ophthalmol*. 1998;126 (6):791–797. doi:10.1016/s0002-9394(98)00242-6
3. Takase N, Nozaki M, Kato A, Ozeki H, Yoshida M, Ogura Y. Enlargement of foveal avascular zone in diabetic eyes evaluated by en face optical coherence tomography angiography. *Retina*. 2015;35(11):2377–2383. doi:10.1097/IAE.0000000000000849
4. Tan CS, Lim LW, Chow VS, et al. Optical Coherence Tomography Angiography Evaluation of the Parafoveal Vasculature and Its Relationship With Ocular Factors. *Invest Ophthalmol Vis Sci*. 2016;57(9):OCT224–34. doi:10.1167/iovs.15-18869
5. Haddouche A, Adel M, Rasigni M, Conrath J, Bourennane S. Detection of the foveal avascular zone on retinal angiograms using Markov random fields. *Digit Signal Process*. 2010;20(1):149–154. doi:10.1016/j.dsp.2009.06.005
6. Bresnick GH, Condit R, Syrjala S, Palta M, Groo A, Korth K. Abnormalities of the foveal avascular zone in diabetic retinopathy. *Arch Ophthalmol*. 1984;102(9):1286–1293. doi:10.1001/archopht.1984.01040031036019
7. Remky A, Wolf S, Knabben H, Arend O, Reim M. Perifoveal capillary network in patients with acute central retinal vein occlusion. *Ophthalmology*. 1997;104(1):33–37. doi:10.1016/s0161-6420(97)30365-0
8. Koulisis N, Kim AY, Chu Z, et al. Quantitative microvascular analysis of retinal venous occlusions by spectral domain optical coherence tomography angiography. *PLoS One*. 2017;12(4):e0176404. doi:10.1371/journal.pone.0176404
9. Kapsala Z, Pallikaris A, Mamoulakis D, Moschandreas J, Bontzos G, Tsilimbaris M. Perifoveal capillary network quantification in young diabetic patients with subclinical or no retinopathy. *Can J Ophthalmol*. 2018;53(3):199–206. doi:10.1016/j.jcjo.2017.09.029
10. Tam J, Martin JA, Roorda A. Noninvasive visualization and analysis of parafoveal capillaries in humans. *Invest Ophthalmol Vis Sci*. 2010;51 (3):1691–1698. doi:10.1167/iovs.09-4483
11. Popovic Z, Knutsson P, Thaung J, Owner-Petersen M, Sjöstrand J. Noninvasive imaging of human foveal capillary network using dual-conjugate adaptive optics. *Invest Ophthalmol Vis Sci*. 2011;52(5):2649–2655. doi:10.1167/iovs.10-6054
12. Conrath J, Giorgi R, Raccah D, Ridings B. Foveal avascular zone in diabetic retinopathy: quantitative vs qualitative assessment. *Eye*. 2005;19 (3):322–326. doi:10.1038/sj.eye.6701456
13. Schottenhamml J, Moult EM, Ploner S, et al. An automatic, intercapillary area-based algorithm for quantifying diabetes-related capillary dropout using optical coherence tomography angiography. *Retina*. 2016;1(Suppl 1):S93–S101. doi:10.1097/IAE.0000000000001288
14. Mondal PP, Rajan K, Ahmad I. Filter for biomedical imaging and image processing. *J Opt Soc Am a Opt Image Sci Vis*. 2006;23(7):1678–1686. doi:10.1364/josaa.23.001678
15. Frangi AF, Niessen WJ, Vincken KL, Viergever MA, "Multiscale vessel enhancement filtering. In: Proceedings of medical image comput assisted intervention (MICCAI)," *Lecture notes in computer science 1496*; 1998. 130–137.
16. Myles PS, Cui J. Using the Bland-Altman method to measure agreement with repeated measures. *Br J Anaesth*. 2007;99(3):309–311. doi:10.1093/bja/aem214
17. Bland JM, Altman DG. Measurement error. *BMJ*. 1996;313(7059):744. doi:10.1136/bmj.313.7059.744
18. Zou GY. Confidence interval estimation for the Bland-Altman limits of agreement with multiple observations per individual. *Stat Methods Med Res*. 2013;22(6):630–642. doi:10.1177/0962280211402548
19. Bland JM, Altman DG. Statistical methods for assessing agreement between two methods of clinical measurement. *Lancet*. 1986;1(8476):307–310.
20. Carstensen B. 2010. *Comparing Clinical Measurement Methods: A Practical Guide*. Chichester, UK: Wiley, Chapter 11.1; ISBN 978-0-470-69423-7.
21. Lopes de Faria JM, Andreazzi Duarte D, Larico Chavez RF, Arthur AM, Arthur R, Iano Y. Reliability and validity of digital assessment of perifoveal capillary network measurement using high-resolution imaging. *Br J Ophthalmol*. 2014;98(6):726–729. doi:10.1136/bjophthalmol-2013-304100
22. Kim DY, Fingler J, Zawadzki RJ, et al. Noninvasive imaging of the foveal avascular zone with high-speed, phase-variance optical coherence tomography. *Invest Ophthalmol Vis Sci*. 2012;53(1):85–92. doi:10.1167/iovs.11-8249
23. Matsunaga D, Yi J, Puliafito CA, Kashani AH. OCT angiography in healthy human subjects. *Ophthalmic Surg Lasers Imaging Retina*. 2014;45 (6):510–515. doi:10.3928/23258160-20141118-04
24. Tam J, Dhamdhere KP, Tiruveedhula P, et al. Subclinical capillary changes in non-proliferative diabetic retinopathy. *Optom Vis Sci*. 2012;89(5): E692–703. doi:10.1097/OPX.0b013e3182548b07
25. Garcia JM, Lima TT, Louzada RN, Rassi AT, Isaac DL, Avila M. Diabetic Macular Ischemia Diagnosis: comparison between Optical Coherence Tomography Angiography and Fluorescein Angiography. *J Ophthalmol*. 2016;2016:3989310. doi:10.1155/2016/3989310
26. Tam J, Dhamdhere KP, Tiruveedhula P, et al. Disruption of the retinal parafoveal capillary network in type 2 diabetes before the onset of diabetic retinopathy. *Invest Ophthalmol Vis Sci*. 2011;52(12):9257–9266. doi:10.1167/iovs.11-8481
27. Li X, Yu Y. Quantitative analysis of retinal vessel density and thickness changes in diabetes mellitus evaluated using optical coherence tomography angiography: a cross-sectional study. *BMC Ophthalmol*. 2021;21:259. doi:10.1186/s12886-021-01988-2
28. Ma Y. ROSE: a Retinal OCT-Angiography Vessel Segmentation Dataset and New Model. *IEEE Trans Med Imaging*. 2021;40(3):928–939. doi:10.1109/TMI.2020.3042802
29. Martínez-Río J, Carmona EJ, Cancelas D, Novo J, Ortega M. Robust multimodal registration of fluorescein angiography and optical coherence tomography angiography images using evolutionary algorithms. *Comput Biol Med*. 2021;134:104529. doi:10.1016/j.compbiomed.2021.104529
30. Sun G, Liu X, Yu X. Multi-path cascaded U-net for vessel segmentation from fundus fluorescein angiography sequential images. *Comput Methods Programs Biomed*. 2021;211:106422. doi:10.1016/j.cmpb.2021.106422
31. Conti G, Postelmans L, Dorchy H. Screening for diabetic retinopathy with fluorescein angiography in patients with type 1 diabetes from adolescence to adult life. A retrospective study of the past 30 years of clinical practice in a tertiary Belgian centre. *Endocrinol Diabetes Metab*. 2022;5(1):e00304. doi:10.1002/edm2.304
32. Ashraf M, Wagdy W, Tawfik MA, Ahmed ISH, Souka A. Potential impact of fluorescein angiography as a primary imaging modality in the management of diabetic retinopathy. *Indian J Ophthalmol*. 2022;70(10):3579–3583. doi:10.4103/ijo.IJO_641_22

33. Elrashidy HE, Samir G. Optical coherence tomography angiography in comparison with fluorescein angiography in diabetic retinopathy. *J Med Sci Res*. 2022;5:187–193.
34. Bawany MH, Ding L, Ramchandran RS, Sharma G, Wykoff CC, Kuriyan AE. Automated vessel density detection in fluorescein angiography images correlates with vision in proliferative diabetic retinopathy. *PLoS One*. 2020;15(9):e0238958. doi:10.1371/journal.pone.0238958
35. Abbasnejad A, Tomkins-Netzer O, Winter A, et al. A fluorescein angiography-based computer-aided algorithm for assessing the retinal vasculature in diabetic retinopathy. *Eye*. 2022. doi:10.1038/s41433-022-02120-4
36. Nunez JM, Sen P, Rasheed R, et al. Deep Learning-Based Segmentation and Quantification of Retinal Capillary Non-Perfusion on Ultra-Wide-Field Retinal Fluorescein Angiography. *J Clin Med*. 2020;9(8):2537. doi:10.3390/jcm9082537
37. Gao Z, Pan X, Shao J, et al. Automatic interpretation and clinical evaluation for fundus fluorescein angiography images of diabetic retinopathy patients by deep learning. *Br J Ophthalmol*. 2022. doi:10.1136/bjo-2022-321472
38. Gao Z, Jin K, Yan Y, et al. End-to-end diabetic retinopathy grading based on fundus fluorescein angiography images using deep learning. *Graefes Arch Clin Exp Ophthalmol*. 2022;260(5):1663–1673. doi:10.1007/s00417-021-05503-7
39. Young LH, Kim J, Yakin M, et al. Automated Detection of Vascular Leakage in Fluorescein Angiography - A Proof of Concept. *Transl Vis Sci Technol*. 2022;11(7):19. doi:10.1167/tvst.11.7.19
40. Guo Y, Hormel TT, Xiong H, et al. Development and validation of a deep learning algorithm for distinguishing the nonperfusion area from signal reduction artifacts on OCT angiography. *Biomed Opt Express*. 2019;10(7):3257–3268. doi:10.1364/BOE.10.003257
41. Iafe NA, Phasukkijwatana N, Chen X, Sarraf D. Retinal Capillary Density and Foveal Avascular Zone Area Are Age-Dependent: quantitative Analysis Using Optical Coherence Tomography Angiography. *Invest Ophthalmol Vis Sci*. 2016;57(13):5780–5787. doi:10.1167/iovs.16-20045
42. Garrity ST, Iafe NA, Phasukkijwatana N, Chen X, Sarraf D. Quantitative Analysis of Three Distinct Retinal Capillary Plexuses in Healthy Eyes Using Optical Coherence Tomography Angiography. *Invest Ophthalmol Vis Sci*. 2017;58(12):5548–5555. doi:10.1167/iovs.17-22036
43. Coscas F, Sellam A, Glacet-Bernard A, et al. Normative Data for Vascular Density in Superficial and Deep Capillary Plexuses of Healthy Adults Assessed by Optical Coherence Tomography Angiography. *Invest Ophthalmol Vis Sci*. 2016;57(9):OCT211–23. doi:10.1167/iovs.15-18793
44. Yu PK, Mehnert A, Athwal A, Sarunic MV, Yu DY. Use of the Retinal Vascular Histology to Validate an Optical Coherence Tomography Angiography Technique. *Transl Vis Sci Technol*. 2021;10(1):29. doi:10.1167/tvst.10.1.29
45. Zheng Y, Gandhi JS, Stangos AN, Campa C, Broadbent DM, Harding SP. Automated segmentation of foveal avascular zone in fundus fluorescein angiography. *Invest Ophthalmol Vis Sci*. 2010;51(7):3653–3659. doi:10.1167/iovs.09-4935
46. Bunce C, Stratton IM, Elders A, Czanner G, Doré C, Freemantle N; Ophthalmic Statistics Group. Ophthalmic statistics note 13: method agreement studies in ophthalmology-please don't carry on correlating. *Br J Ophthalmol*. 2019;103(9):1201–1203. doi:10.1136/bjophthalmol-2018-313759

Clinical Ophthalmology Dovepress

Publish your work in this journal

Clinical Ophthalmology is an international, peer-reviewed journal covering all subspecialties within ophthalmology. Key topics include: Optometry; Visual science; Pharmacology and drug therapy in eye diseases; Basic Sciences; Primary and Secondary eye care; Patient Safety and Quality of Care Improvements. This journal is indexed on PubMed Central and CAS, and is the official journal of The Society of Clinical Ophthalmology (SCO). The manuscript management system is completely online and includes a very quick and fair peer-review system, which is all easy to use. Visit http://www.dovepress.com/testimonials.php to read real quotes from published authors.

Submit your manuscript here: https://www.dovepress.com/clinical-ophthalmology-journal